

4 Enabling the Discovery of Kilonovae Associated with Neutron Star Mergers with Electromagnetic Follow-up

5 MARIANNA PEZZELLA, TOMÁS AHUMADA, AND SHREYA ANAND

6 ABSTRACT

7 The Laser Interferometer Gravitational-Wave Observatory (LIGO) is designed to detect gravitational  
8 waves (GWs) produced by events such as merging neutron stars or black holes (BHs). The first  
9 detection of GWs and electromagnetic radiation (EMR) from a binary neutron star (BNS) merger  
10 occurred on August 17, 2017, with the discovery of GW170817. The merger was followed by a kilonova  
11 (KN), responsible for the synthesis of heavy elements, beyond iron, in the universe. During LIGO's  
12 fourth observing run, O4, ZTF produces candidates for which photometric and spectroscopic data  
13 analysis are performed. This candidate vetting aims to uncover the KN counterpart associated with  
14 a particular GW event. The DRAGONS (Data Reduction for Astronomy from Gemini Observatory  
15 North and South) pipeline will be used to re-analyze the spectrum of GW170817 that was taken with  
16 Gemini Multi-Object Spectrograph (GMOS). We adapt the DRAGONS pipeline to include black-body  
17 curve fitting and spectroscopic line identification for potential candidates detected in O4 and future  
18 observing runs. This automated pipeline will help reduce the data and determine the composition  
19 and temperature of KNe. By updating this pipeline, the candidate KNe sample will be analyzed more  
20 quickly and efficiently during transient searches for EM counterparts by eliminating any contaminants,  
21 such as Supernovae (SNe), active galactic nuclei (AGNs), or cataclysmic variables. This method  
22 will enable the detection of early KN emission, which is crucial for studying the synthesis of heavy  
23 elements and understanding the physics of BNS mergers. This data reduction pipeline for photometry  
24 and spectroscopy of KNe during O4 will be used to aid in the real-time study of heavy element  
25 nucleosynthesis.

26 1. INTRODUCTION

27 1.1. LIGO

28 The Laser Interferometer Gravitational-Wave Observa-  
29 tory (LIGO) consists of two identical Michelson inter-  
30 ferometer detectors located in Hanford, Washington,  
31 and Livingston, Louisiana, with each detector consist-  
32 ing of two, four-kilometer long, L-shaped arms<sup>1</sup>. This  
33 observatory was built to study ripples in spacetime, or  
34 gravitational waves (GWs). GWs are the bending of  
35 space and time; as space is stretched in one direction, it  
36 is compressed in the perpendicular direction simultane-  
37 ously. As this happens, one arm of the interferometer  
38 gets shorter and the other gets longer as the GW is  
39 passing. Although these changes are minute, the observa-  
40 tory is designed to detect these alterations. Since the  
41 lengths of the arms are changing in opposing ways, or  
42 differentially, this motion is called Differential Arm mo-

43 tion, or differential displacement<sup>1</sup>. Similar to the length  
44 of the arms, the length of the laser beams also become  
45 longer and shorter with the passing of the wave, causing  
46 an oscillation pattern. These oscillations interact with  
47 the beamsplitter inside the interferometer and are out  
48 of alignment when they hit the beamsplitter due to the  
49 GW. A voltage signal will then be emitted from the in-  
50 terferometer as a result of this event. The GWs events  
51 that LIGO is sensitive to are caused by events such as  
52 mergers of binary neutron stars (BNSs), neutron stars-  
53 black holes (NSBHs), or binary black holes (BBHs).  
54 There have been numerous upgrades on the detector,  
55 mainly to upgrade sensitivity<sup>2</sup>. The most prominent  
56 source of uncertainty for the detectors is noise. Various  
57 noise sources, such as laser, seismic, angular controls,  
58 and residual gas noise cause false detections almost ev-  
59 ery day. One of the best ways found to combat these  
60 detrimental noise sources is to have two detectors at  
61 different sites, thus reducing localization errors. There-

Corresponding author: Marianna Pezzella  
PEZZELM1@my.erau.edu

<sup>1</sup> <https://www.ligo.caltech.edu/>

<sup>2</sup> <https://www.virgo-gw.eu/science/detector/>

62 fore, if only one detector picks up a signal, it is discarded,  
 63 but if both locations detect the same signal at the same  
 64 time, it is regarded as an event. Multiple observing runs  
 65 have been completed with both the LIGO and Virgo detec-  
 66 tors. Virgo is one of LIGO’s sister facilities, located  
 67 in Cascina, Italy<sup>3</sup>. This facility is similar to the LIGO  
 68 setup with two perpendicular arms and a beamsplitter  
 69 inside the interferometer<sup>3</sup>. Together, using triangulation  
 70 for source identification, these facilities have discovered  
 71 many binary mergers, thus supporting Einstein’s theory  
 72 of general relativity.

### 73 1.2. Binary Mergers

74 There are two main types of mergers that will be fo-  
 75 cused on in this paper: BNSs and NSBHs. A binary  
 76 merger is when two very massive bodies orbit around  
 77 each other and the same center of mass for the system,  
 78 gain angular acceleration due to the gravitational fields  
 79 of each object, and eventually collide with each other  
 80 in an extremely energetic event. There are three stages  
 81 of these events in which GWs are expelled: the inspi-  
 82 ral, the merger, and the ringdown. Figure 1 shows these  
 83 defining stages of the GW merger event.

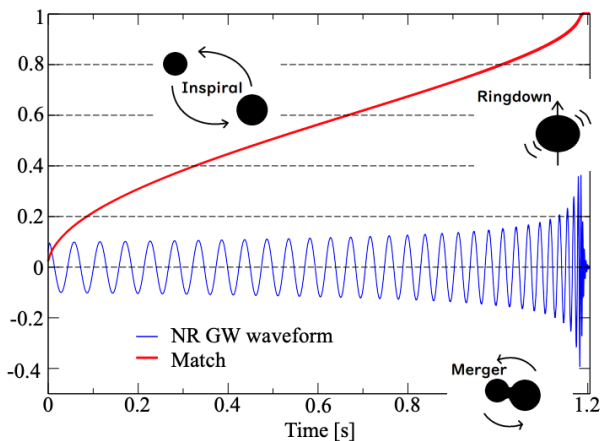


**Figure 1.** Binary merger process with the GW waveform. Figure from (Isoyama et al. 2021).

84 A BNS merger is ultimately a collision of the two mas-  
 85 sive neutron stars in the binary system. The detection  
 86 of NSBH mergers has been much more rare, but still  
 87 plausible. While a BNS merger will either merge into a  
 88 larger neutron star or a black hole (BH), a NSBH and  
 89 BBH merger will both merge into a BH (Abbott et al.  
 90 2017). These enormously dense and massive objects col-  
 91 lide, triggering a flash of light that is caused by matter

<sup>3</sup> <https://www.virgo-gw.eu/science/detector/>

92 ejected from the collision. LIGO and Virgo can detect  
 93 the GWs from these collisions. Up until the start of this  
 94 project, two BNSs and two NSBHs have been confirmed  
 95 (The LIGO Scientific Collaboration et al. 2021).

### 96 1.3. GW170817

97 On August 17, 2017, the LIGO and Virgo detec-  
 98 tors discovered the first GWs from the BNS merger:  
 99 GW170817. Figure 2 shows the GWs detected.

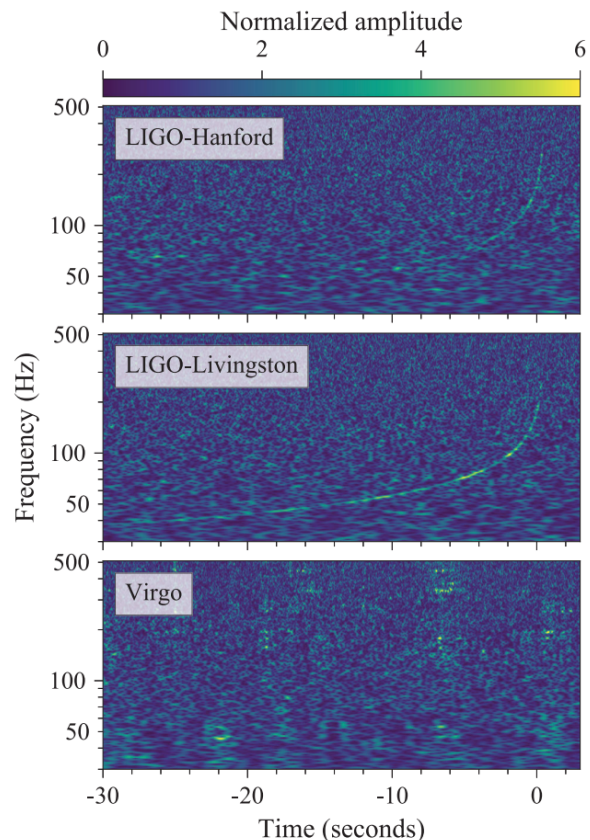


**Figure 2.** LIGO data from the GW170817 event. Figure from Abbott et al. (2017).

100 Almost simultaneously, the Fermi and Integral satel-  
 101 lites detected electromagnetic radiation (EMR) in the  
 102 form of gamma-rays through the multi-wavelength ob-  
 103 servation that took place (Goldstein et al. 2017) This  
 104 was a landmark event in the history of astrophysics. The  
 105 chirp mass of this system was measured to be

$$M_C \equiv \frac{(M_1 M_2)^{3/5}}{(M_1 + M_2)^{1/5}} \simeq 1.118 M_\odot \quad (1)$$

106 The signal to noise ratio (SNR) from this event was  
 107 about 32.4 (Abbott et al. 2017). The event, which oc-  
 108 curred on LIGO’s second observing run (O2), was about

109 40 Megaparsecs away (Abbott et al. 2017). GW170817  
 110 was one of the most studied events in the history of  
 111 physics and astronomy. The BNS merger lit up an im-  
 112 mensely wide range of frequencies that were detectable  
 113 on the entire electromagnetic (EM) spectrum.

114 When the gravitational pull from two exceedingly  
 115 dense objects in a binary system begins to angularly  
 116 accelerate the bodies around each other, they begin to  
 117 collapse inwards. A merger occurs when the two objects  
 118 finally collide and a large amount of energy is released  
 119 in the form of gravitational waves and radiation. For  
 120 a BNS merger such as GW170817, additional energy is  
 121 released as EMR: first as a gamma-ray burst (GRB) and  
 122 later in the form of a kilonova (KN). A KN is the EM  
 123 transient powered by the radioactive decay of heavy el-  
 124 ements produced during the merger. Figure 3 shows an  
 125 overview on a KN.

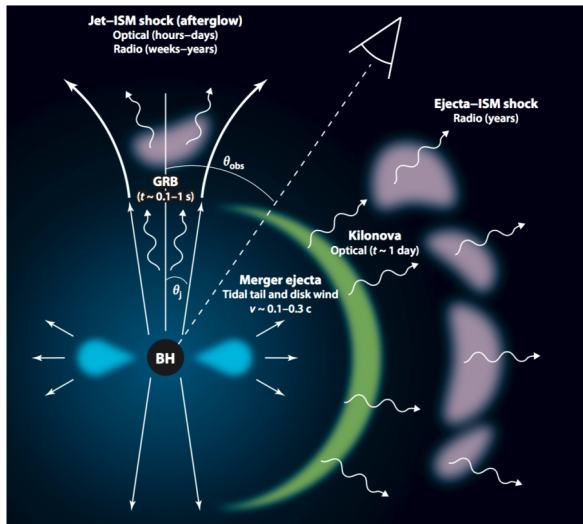


**Figure 3.** Overview of the process of a KN. Figure from Metzger (2019).

126 A GRB is one of the most energetic events in the uni-  
 127 verse, consisting of a jet of high-energy, in this case a  
 128 byproduct of the collision. There are two types of GRBs:  
 129 a short gamma ray burst (SGRB) and a long gamma  
 130 ray burst (LGRB). A SGRB is categorized as lasting  
 131 shorter than two seconds, and is usually associated with  
 132 KNe, while a LGRB is categorized to last longer than  
 133 two seconds, and is usually associated with supernovae  
 134 (SNe). Recently, astronomers have questioned this cat-  
 135 egorization due to observations of a LGRB seeming to  
 136 have come from a KN. Figure 4 shows two overlapping  
 137 Gaussian curves which represent the SGRB and LGRB  
 138 categories accepted by astronomers today.

139 The first detection of EMR from the GW170817  
 140 merger was a burst of gamma-ray emission approxi-

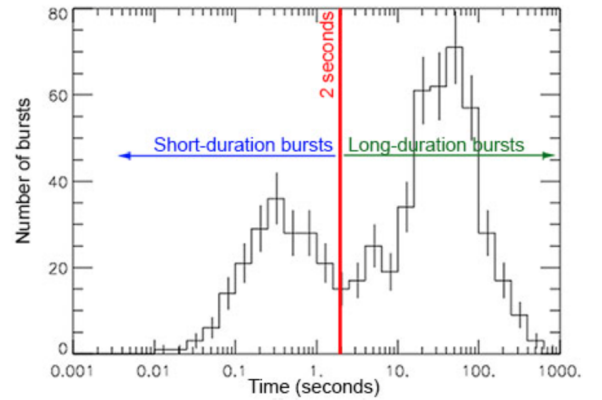


**Figure 4.**

Observed GRB from the BATSE instrument on the  
 Compton Gamma-ray Telescope<sup>a</sup>.

<sup>a</sup><https://imagine.gsfc.nasa.gov/science/objects/bursts1.html>

141 mately 1.7 seconds after the inspiral ended (Metzger  
 142 2019). Other types of EMR could not be detected at  
 143 such early times. X-ray luminosity was detected after  
 144 about 2.3 days (Metzger 2019). There are many com-  
 145 ponents of a KN, such as the tidal and wind compo-  
 146 nents of the ejecta. Tidal ejecta results from the tidal  
 147 forces experienced by the neutron stars during the mer-  
 148 ger, while wind ejecta is produced by the high-speed  
 149 winds that emanate from the merged object (Perego et al.  
 150 2021). KNe directly relate to the synthesis of heavy  
 151 elements. The rapid neutron-capture process, or  $r$ -  
 152 process, is the primary process by which heavy elements  
 153 beyond iron are synthesized in the universe (Perego  
 154 et al. 2021). During the  $r$ -process, heavy atomic nu-  
 155 clei are created through rapid neutron capture followed  
 156 by beta decays, synthesizing heavy elements such as  
 157 gold, platinum, and uranium (Perego et al. 2021). The  
 158 GW170817 merger was an example of direct evidence  
 159 of  $r$ -process nucleosynthesis. The KN associated with  
 160 this event, produced by the radioactive decay of heavy  
 161 elements synthesized in the  $r$ -process, displayed a multi-  
 162 component light curve, consisting of both red and blue  
 163 components, which are attributed to different physical  
 164 processes. The peak energy of the radiation can vary  
 165 depending on the composition of the ejecta, generating  
 166 either a red, blue, or mixed kilonova. (Metzger 2019).  
 167 Studying these light curve components will allow us to  
 168 understand more about the KN and  $r$ -process in each  
 169 particular merger (Metzger 2019).

#### 170 1.4. ZTF: Finding the optical counterpart

171 The Zwicky Transient Facility (ZTF) is a time-domain  
 172 astronomy project mounted on the Palomar 48-inch tele-  
 173 scope that surveys the entire northern night-sky every

three nights. This telescope searches for transient events such as SNe, active galactic nuclei (AGNs), and variable stars. ZTF has also dedicated an extensive amount of effort to finding the precise location of compact mergers, looking through short GRB localizations (Ahumada et al. 2022a), and through the follow up of GW events. When a GW event is detected, LIGO releases an alert stating the properties of the merger. Usually, the large localization errors have prevented the community from pinpointing GW events. However, the large field-of-view (FOV) of ZTF has allowed for effective searches in the past (Kasliwal et al. 2020). ZTF has a FOV of 47 square degrees and an areal survey rate of 3750 square degrees per hour<sup>4</sup>. These specifications make ZTF an essential piece of equipment for searching large portions of the sky in short times; it is the only telescope of its kind today. Some of the filters that potential candidates need to pass through in order to become an “interesting” candidate are to: be spatially coincident, have positive subtraction, be real, have no star underneath, have no bright nearby star, not be a moving object, have previous history, have lightcurve data, have color evolution, have magnitude evolution, not be a AGN, and be consistent with the GW distance. For many potential candidates, there are reference images that will be subtracted with the new image when ZTF is triggered on an event. This subtraction must be positive, meaning they must have a remnant after the subtraction. Stars near the potential candidates can complicate observations due to saturation issues and differentiating between the sources. Lightcurve and magnitude evolution are filters based on specific properties of the candidate. In relation to the color evolution of a candidate, astronomers are looking for red candidates. This means they are fast fading and give off light closer to the infrared part of the spectrum, which has been proven to coincide with KN counterparts. ZTF, the Multi-Messenger Astronomy (MMA) group, and other scientists will process the potential candidates and determine the coordinates of an event, if there seems to be a promising candidate for the event. The data is then passed along to larger telescopes such as the Gemini or Keck observatories for deeper observations using both spectroscopy and photometry<sup>4</sup>. By combining the spectroscopic data from larger facilities, photometric data from ZTF, and data from LIGO, physicists and astronomers can get a more complete understanding of MMA events and their properties.

<sup>4</sup> <https://www.ztf.caltech.edu/>

## 1.5. Photometry vs. Spectroscopy

Photometry and spectroscopy are two of the most important techniques used by astronomers to study celestial objects across the universe. More recently, these techniques have been used for detecting and analyzing BNS and NSBH mergers. Photometry involves measuring the intensity of light from an astronomical object, typically across a range of wavelengths, to obtain information about its brightness, color, and variability (Abbott et al. 2017). This information can be used to study a wide range of phenomena, from the orbits of exoplanets around distant stars to the properties of distant galaxies. Spectroscopy involves separating the light from an astronomical object into its component wavelengths to obtain a spectrum that can be used to study the object’s composition, temperature, motion, and other physical properties (Abbott et al. 2017). Spectroscopy can be used to identify the chemical elements present in stars and galaxies, measure their velocities, and study the physical processes that are occurring within them.

While both photometry and spectroscopy are vital to furthering our understanding and analysis of GWs, they both provide different types of information. Photometry is useful for studying the overall brightness and variability of an object, while spectroscopy provides detailed information about the object’s physical properties. Both techniques are often used in conjunction with each other to obtain a more complete understanding of celestial bodies and complex astronomical events. These two techniques are complementary, and they are essential to furthering and advancing our understanding of BNS and NSBH mergers and of the signatures of r-process nucleosynthesis.

## 2. GW ALERTS DURING O4

### 2.1. S230627c

During the first week of this project, both LIGO Hanford and Livingston detected an event called S230627c, during which the MMA group tasks and the process for analyzing candidates and triggering ZTF was shown. This event was initially recorded as 49% NSBH and 48% BBH<sup>5</sup>. The MMA group began to analyze the data from this event, making decisions on how to proceed for further analysis. Since there was a chance that this event could potentially be a NSBH, the group began discussing the incoming data from the trigger. There was only a small chance, about 11%, of it being in the *massgap*. The *massgap* is the gap in mass between the heaviest

<sup>5</sup> <https://gracedb.ligo.org/superevents/public/O4/>

270 neutron stars (about 2.5 solar masses) and the lightest  
 271 BHs (about 5 solar masses), where there have not been  
 272 many binary mergers found<sup>6</sup>. The area was well local-  
 273 ized, about 50% spanned only 20 square degrees, had a  
 274 very high significance, and had a false alarm rate (FAR)  
 275 of less than 1 per 100.04 years. Figure 5 shows the local-  
 276 ization of S230627c. The lower part of the localization  
 277 was relatively near to the sun, so it was below 30 de-  
 278 grees at twilight, close to an airmass (a measure of the  
 279 atmospheric air in the line of sight of the observer) of  
 280 about two.

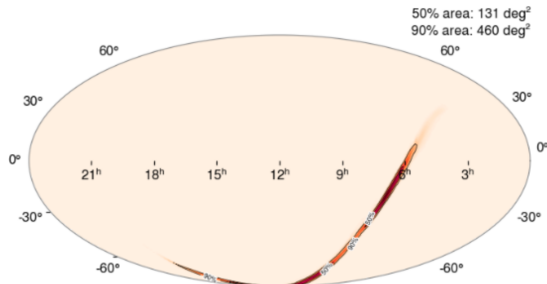


Figure 5. Localization are of S230627c. Figure from<sup>a</sup>.

<sup>a</sup><https://fritz.science/>

281 This event, after preliminary observations, was a go  
 282 for a full response from ZTF and WINTER. ZTF was  
 283 triggered and began searching for candidates for the EM  
 284 counterpart. The event was most likely a BBH since the  
 285 physical limit for a neutron star is heavier than 2.2 solar  
 286 masses, when it collapses gravitationally and becomes a  
 287 BH. However, it was so well localized and had too good  
 288 of a FAR to stop searching. A lot of the analysis for  
 289 BNS and NSBH candidates is completed through Fritz.  
 290 Fritz is an open source code designed for time-domain  
 291 astronomers to use for collaboration on a project<sup>7</sup>. ZTF  
 292 observed the localization region for  $\sim 3$  hours, and can-  
 293 didates started to appear on Fritz for further scrutiny.  
 294 The candidates needed to be evolving quickly. Unfor-  
 295 tunately, none of the candidates were very compelling,  
 296 but to maximize the scientific gains, ZTF observed the  
 297 following night as well. The search ultimately covered  
 298 74.9 %, or 91.5 square degrees, of the reported localiza-  
 299 tion region. Throughout this process, a log journal was  
 300 kept to further review the steps of candidate analysis  
 301 afterwards. The log took special note of certain terms  
 302 or phrases used and commonly used platforms to further  
 303 explore.

<sup>6</sup> <https://www.caltech.edu/about/news/ligo-virgo-finds-myste-ry-object-mass-gap>

<sup>7</sup> <https://fritz.science/about>

## 2.2. S230808i

304 For this detection, there was a good significance, but  
 305 the localization area was very large. The MMA group  
 306 began to discuss the properties of the event. Origin-  
 307 ally, there was debate about this event possibly being a  
 308 BBH, but since the source classification was incomplete  
 309 and the ZTF fields were visible right away from Palo-  
 310 mar, the group decided to trigger ZTF. A few candi-  
 311 dates started to appear after initial scanning from ZTF.  
 312 Forced photometry was performed on the eight candi-  
 313 dates and eventually ruled out most of them. There  
 314 was one intriguing candidate for which spectroscopy and  
 315 photometry were requested. One of the interesting can-  
 316 didates was determined to be an AGN based on its alpha  
 317 features. Later that night, this event was retracted after  
 318 pipeline experts reviewed the trigger and determined it  
 319 was of low significance.  
 320

## 3. PIPELINE OBJECTIVES

321 This MMA project will be used to develop pipelines  
 322 for spectroscopic and photometric data analysis. The  
 323 current pipeline for Gemini was used to observe the EM  
 324 signatures from GW170817. There will be many more  
 325 candidates for Gemini in the ongoing and upcoming ob-  
 326 serving runs, so a more streamlined process for analyzing  
 327 the Gemini data is needed. Therefore, astronomers are  
 328 in need of a more sophisticated and novel data analysis  
 329 pipeline to extract information from the large and com-  
 330 plex datasets generated by instruments like LIGO and  
 331 Gemini.  
 332

333 The first task will be to run the Data Reduction for  
 334 Astronomy from Gemini Observatory North and South  
 335 (DRAGONS) pipeline with a sample data set to pro-  
 336 duce a spectrum and overlay spectral lines on the plot.  
 337 A novel pipeline will then be created by updating and  
 338 adapting the DRAGONS pipeline. This novel pipeline  
 339 will be able to reproduce the spectral features of the KN  
 340 associated with GW170817. The novel pipelines will be  
 341 developed originally for Gemini, but will also be recre-  
 342 ated for other infrared facilities. Additionally, the novel  
 343 pipelines will have another part worked into their cod-  
 344 ing. While the previous pipelines were only able to uti-  
 345 lize spectroscopic data, the novel pipelines will utilize  
 346 photometric data as well. This addition will give as-  
 347 tronomers more ways to analyze the data from LIGO  
 348 detections.

349 Some of the instruments used for reducing the data  
 350 using spectroscopic and photometric pipelines are the  
 351 Las Cumbres Observatory (LCO), Gemini Observa-  
 352 tory, and Southern Astrophysical Research Telescope  
 353 (SOAR). LCO uses photometry with its Sinistro (1-  
 354 meter), Spectral (2-meter) and MuSCAT3 (2-meter)

cameras<sup>8</sup>. FLAMINGOS-2 is a near-infrared imaging spectrograph at Gemini-South, which utilizes photometry and spectroscopy to gather more in-depth data from merger events<sup>9</sup>. DRAGONS is a package used in conjunction with the Gemini Multi-Object Spectrograph (GMOS) to reduce data. This project will rely heavily on the DRAGONS tutorial to modify and adapt the proposed automated pipeline. The Southern Astrophysical Research Telescope (SOAR) uses both photometry and spectroscopy to produce high image quality at wavelengths from optical to near-infrared<sup>10</sup>. The Goodman spectrograph is an optical imitating spectrograph<sup>10</sup>. Both the FLAMINGOS-2 telescope from the Gemini Observatory and the SOAR telescope are both located on the same mountain. Documentation and data from these instruments will be gathered to formulate the pipeline which will be able to reproduce the data collected from GW170817.

Currently, there is a reduction pipeline provided at these observatories. This project will explore these pipelines and then adapt them using the new parameters for the specific program. This includes ensuring there is an automated pipeline that downloads raw data, calibrates it, performs image subtraction, robustly gets the photometry for each image, and uploads it to Fritz. This will be the case for the LCO imaging pipeline, especially with imaging subtraction and photometry. A plan will be created to build and test a near-infrared spectroscopic data reduction pipeline for the DRAGONS Gemini Observatory Archive<sup>11</sup> to reproduce the features in the spectra shown in [Watson et al. \(2019\)](#). For the spectroscopic image calibration of all the pipelines, darks, flat fields, arcs, and biases will be needed to process the spectra<sup>11</sup>.

When a GW event is detected by LIGO, ZTF is notified and begins scanning for candidates of the EM counterpart (the KN). This search takes time because of the limited astronomy equipment in today's society, which is deficient in both abundance and technological advancement for the tasks it is expected to execute. However, the search is time sensitive since KNe are incredibly fast fading. Compared to SNe and AGNs, KNe will fade optically in just a few days while SNe and AGNs may last a few weeks. The counterpart should be highly redshifted, meaning the source is moving away from the Earth. The velocity of the ejecta will result in the surrounding mate-

rial from the explosion moving towards the Earth. The ejecta needs to have a high velocity for it to be a KN. There are four main ways to analyze the KNe which allow for a more detailed look into the KN: optical photometry, infrared photometry, optical spectroscopy, and infrared spectroscopy. This project aims to gather data within all four categories to gain the most accurate representation of the KN. Optical photometry helps to analyze the candidates; by studying their brightness decay rate, candidates can be ruled out based on how fast-fading their counterpart is. The infrared photometry component of the KN is expected to last longer, so it will provide more detail than optical photometry. Optical spectroscopy will measure the temperature and redshift of the ejecta ([Valeev et al. 2021](#)). The temperature is directly related to the abundance of heavy elements. Assumptions about the KN can be made when certain elements are present in the spectrum. A KN with heavy elements will be hotter in the infrared. The more electrons that are present, the more light can be absorbed. Electrons only absorb a specific wavelength, and since heavier elements absorb more light in the optical ultraviolet spectrum, it cannot be seen by human observers, but it can be seen when it is re-emitted in the infrared. This is why an abundance of heavy elements is assumed when bright infrared emissions are detected. Infrared spectroscopy will compare the r-process nucleosynthesis between elements and how much of each element is being created. While spectroscopic classification is usually preferred overall to rule out transients, photometric classification gives their essential fading rate and color evolution ([Ahumada et al. 2022b](#)).

The software and platforms, such as Anaconda, Visual Studio Code (VSC), Fritz, Jupyter notebook, and Github, provided a learning curve, and took time to understand. The majority of this project was then being able to use these platforms and learn how the DRAGONS pipeline functioned. This was a challenging and time-consuming process, but it ended up helping drastically in the long run.

## 4. METHODS

### 4.1. DRAGONS pipeline

FLAMINGOS-2 is a near-infrared instrument mounted at the Gemini south telescope. In order to analyze the data taken with this instrument, the Gemini observatory has a data processing pipeline; there are tutorials on how to use this pipeline. The following steps are from the F2 Longslit Tutorial in the FLAMINGOS-2 guide<sup>11</sup>. The proper packages for the FLAMINGOS-2 pipeline were installed. Anaconda is a data science platform which was used in conjunction with the python coding

<sup>8</sup> <https://lco.global/observatory/instruments/>

<sup>9</sup> <http://www.gemini.edu/instrumentation/flamingos-2>

<sup>10</sup> <https://noirlab.edu/public/programs/ctio/soar-telescope/>

<sup>11</sup> <https://gemini-iraf-flamingos-2-cookbook.readthedocs.io/en/latest/index.html>

software. This platform was installed, and the data for the pipeline was retrieved. An observations log was created and the reduction and observation log python files were downloaded. The data and the files were all configured and placed in their corresponding folders. After a slight modification of plan due to the desire to focus more on optical photometry and spectroscopy instead of infrared spectroscopy, work with the DRAGONS pipeline began. DRAGONS is another pipeline used by the Gemini Observatory. Two of the main platforms utilized throughout this process were VSC and DRAGONS. The VSC software was used to reconstruct and then develop and refine the pipelines. DRAGONS provided the tools to reduce photometric and spectroscopic data<sup>12</sup>. Example One in the DRAGONS pipeline tutorial was recreated using the following steps on the online tutorials<sup>13</sup>. The Anaconda and DRAGONS packages were added to VSC. To install DRAGONS, the conda-forge and Gemini channel - where the packages needed are located - were added. A virtual environment with the name `dragons` was created. This environment was the location of the DRAGONS software, its dependencies, and Python 3.10, once they were installed. The dragons environment needed to be activated and the proper kernel needed to be selected each time the shell was opened. DRAGONS was configured and then tested to ensure the packages were all installed properly and could be accessed. The `dragonsrc` configuration file was located and opened with an editing software called `nano`. A browser was chosen to be used, and a path and name for the configurations database were created. The `astrodata` and the `gemini-instruments` packages were imported using the python interpreter. A function to reduce the data was defined with python; this function was called the Recipe. A test to ensure that the reduce function runs was carried out. In order to test the installation, data was downloaded from the DRAGONS tutorial section: Downloading tutorial datasets section<sup>12</sup>. The data set for Example One was downloaded for the installation test. After ensuring the DRAGONS environment was activated, the directory where the data files were was opened, and the installation was complete, the set up and calibration for Example One in the DRAGONS tutorial was finished.

There are two different ways to execute the DRAGONS tutorial: through the terminal and through a programming language. Although the execution process for

Example One - Longslit Dithered Point Source - Using the “Reduce” class in DRAGONS was carried out separately utilizing both methods, only the steps to the programming language will be described here as to avoid redundancy. All the work done for Example One was performed in a Jupyter notebook. Jupyter notebook is a interactive computing platform; the terminal and the Python coding language were used in conjunction with the Jupyter notebook in this project. After a Jupyter notebook was created, the path to the downloaded sample data for Example One was opened, the necessary libraries were imported, and the DRAGONS logger was set up. The DRAGONS logger records everything that happens withing the DRAGONS pipeline; it is a record of each error and each command executed. A file lists for all the `.fits` files were created. In the directory where all the data files were stored, each file ending in `.fits` is sorted into a list. DRAGONS uses a calibration database that was initialized to store the path to different calibration files, and besides bias, flats, and arcs, the Bad Pixel Mask (BPM) needs to be manually added to the database. A function to see the shape of each `.fits` file in the directory was carried out and displayed the shapes of each `.fits` file. The Master Bias, Master Flat Field, Processed Arc, and Processed Standard were all reduced and the interactive viewing mode was turned on for them all as well. The specifics of what these four calibration frames do will be further explained in upcoming sections. The reduced, Processed Standard was plotted and displayed. Using the four calibration frames previously mentioned, the Science Observation (SO) was reduced and calibrated. A 2D image of the spectrum was displayed, then the 1-D flux-calibrated spectrum from the main target object was plotted and displayed as well. To get an ascii representation of the spectrum, the primitive `write1DSpectra` was used to extract the values from the `.fits` file. Finally, to use a different format, the format parameters were set.

#### 4.2. *DRAKE pipeline*

The next goal of this project was to upgrade the DRAGONS pipeline by creating a new, more generalized pipeline to reduce data and extract a spectrum for further spectral data analysis. The DRAGONS pipeline was closely followed, but changes were made along the way to produce a generalized pipeline for candidate KNe data reduction. This new pipeline was named DRAKE: Data Reduction for Analysis of Kilonovae Exploration. Most of the reduction and calibration steps for the DRAKE and DRAGONS pipelines are similar, but there were a few changes to make the pipeline more generalized and more efficient. DRAKE has a more up-

<sup>12</sup> [https://dragons.readthedocs.io/projects/gmosls-drtutorial/en/stable/02\\_datasets.html](https://dragons.readthedocs.io/projects/gmosls-drtutorial/en/stable/02_datasets.html)

<sup>13</sup> [https://dragons.readthedocs.io/projects/gmosls-drtutorial/en/v3.1.0/ex1\\_gmosls\\_dithered\\_api.html](https://dragons.readthedocs.io/projects/gmosls-drtutorial/en/v3.1.0/ex1_gmosls_dithered_api.html)

550 to-date comment section, with instructions on where  
 551 to add paths and what parts of the code need to be  
 552 set by the user before starting any kind of analysis.  
 553 A working directory needed to be created, the corre-  
 554 sponding data needed to be downloaded into the work-  
 555 ing directory, the DRAGONS environment needed to be  
 556 set up, and two lines of code needed to be added into  
 557 `dragonsrc` configuration file. The DRAKE pipeline was  
 558 tested using Gemini data of GW170817. In particular,  
 559 the data of the third night was downloaded from the  
 560 Gemini Archive website. Biases, standards, flats, arcs,  
 561 and object images were all downloaded into the working  
 562 directory. These tasks were explained in the first part  
 563 of the DRAKE pipeline. The libraries were imported  
 564 and the DRAGONS logger and calibration service were  
 565 set up and installed. The separate files were all sorted  
 566 into their corresponding lists. The calibration database  
 567 was started and set up properly, and if this had already  
 568 been completed within a previous analysis, an addition  
 569 to the pipeline was made in order to display a message  
 570 stating that the calibration service was already there.  
 571 A loop was created to inspect the data and printed the  
 572 value for the descriptor of interest, the region of inter-  
 573 est (ROI) setting in this case, to inspect the data  
 574 for specific descriptors and to determine how to build  
 575 the `dataselect` expression. The `dataselect` expres-  
 576 sion dictates how the files are selected for various lists.  
 577 There were two sets of biases with different ROI, one set  
 578 of Full Frame biases, and one set of Central Spectrum bi-  
 579 ases, as in with the dataset in Example One, previously  
 580 explained. Depending on the downloaded data, images  
 581 taken could have different binnings, meaning different  
 582 shapes. The biases for the standards that were down-  
 583 loaded in this project had two different binnings, which  
 584 meant the dimensions of the two sets of biases attempt-  
 585 ing to be stacked were not the same. To account for  
 586 this, the DRAKE pipeline was adapted to display each  
 587 of the image shapes and binnings so they could be split  
 588 into their respective lists. The first list had the Cen-  
 589 tral Spectrum biases with 2x2 binnings, and the second  
 590 list had the Central Spectrum biases with 1x2 binnings,  
 591 and the third list had the Full Frame biases. The first  
 592 two lists held the biases for the spectrophotometric stan-  
 593 dards (SSSs), and the third list held the biases for the  
 594 object images (from the SO). Lists for the flats, the arcs,  
 595 and the SO were created separately. For this project,  
 596 images from two different SSSs were downloaded, so the  
 597 DRAKE pipeline was adapted to split the SSS images  
 598 into their corresponding objects and then create their  
 599 own lists. The two SSSs used in this project were object  
 600 "LTT1788" and object "NGC4993-OT."

The calibration database was initialized and the BPM  
 was taken from the calibration database like in the  
 DRAGONS pipeline. Directions to import the neces-  
 sary packages were added to the DRAKE pipeline. To  
 check that the shape of the images in the lists are all  
 consistent, a function was created to read and display  
 the shape of the `.fits` files. A master bias, master flat  
 field, processed arc, and processed standards were re-  
 duced. Where the processed standards were reduced, a  
 few lines of code were added to save those standards  
 as variables to be called upon and used later in the  
 pipeline. To ensure the processed standards were cor-  
 rectly reduced, the pipeline displayed the standards as  
 electron signal vs. wavelength plots and displayed the  
 name of the each standard used to create each plot. The  
 SO for the object, NGC4993-OT in this case, was re-  
 duced and calibrated using a specified standard and the  
 other frames previously mentioned. The 2D spectrum  
 and the 1-D flux-calibrated spectrum of the target were  
 then displayed. A section of code was added to save the  
`1D.fits` file for later analysis as an ascii file.

#### 4.3. Calibration Frames and Processes

There were four frames used for the image calibra-  
 tion in this project. The process of calibration for the  
 DRAKE pipeline utilizing the GW170817 data will be  
 described here. Bias frames (biases), flat frames (flats),  
 arc frames (arcs), and standard frames from a SSS were  
 the four calibration frames utilized. These images are  
 subtracted from the SO, the image taken of the target  
 object being analyzed. Bias frames, or biases, are im-  
 ages taken with no light hitting the imaging sensor to  
 see what dust or grime may be on the sensor itself<sup>14</sup>.  
 This exposure should be taken with the shortest expo-  
 sure time possible. Two sets of bias frames were taken:  
 one for the SSSs and one for the SOs. Since images  
 of both the "Full Frame" (image of the entire object  
 and the "Central Spectrum" (smaller ROI in the center  
 of the CCD) were taken, there will be a bias for both  
 the Full Frame and for the Central Spectrum. Figure  
 6 shows one of the biases used for calibration in the  
 DRAKE pipeline.

Flat frames, or flats, are images taken of something  
 known to be illuminated in the same way throughout  
 the entire frame. A screen can be used as a filter to  
 get symmetric illumination for a flat. Specifically, flats  
 calibrate the light by forcing the illumination to be uni-  
 formly distributed across the image, thus removing any

<sup>14</sup> <https://skyandtelescope.org/astronomy-blogs/imaging-foundations-richard-wright/dark-frames-and-bias-frames-demystified/>



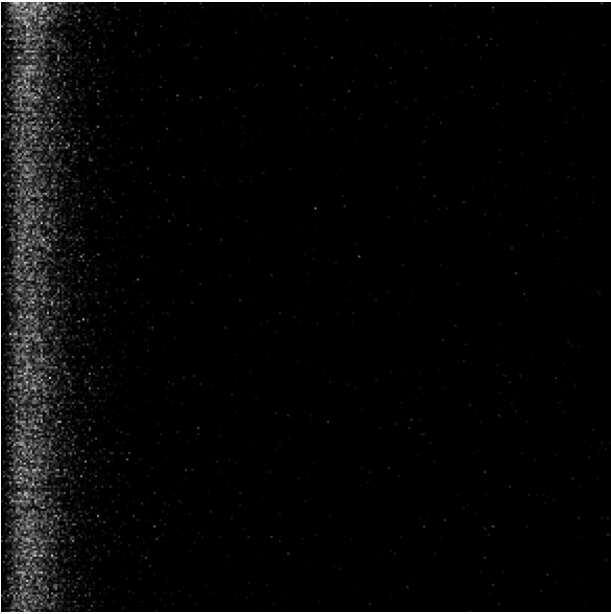


Figure 6. Bias Frame

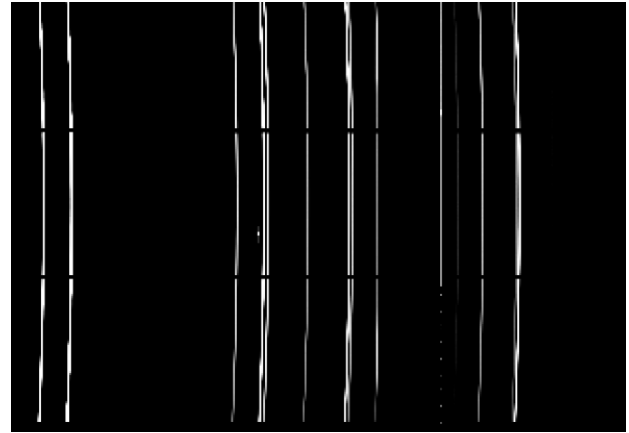


Figure 8. Arc Frame

648 vignetting<sup>15</sup>. Figure 7 shows how an image changes once  
649 flats calibrate the image.

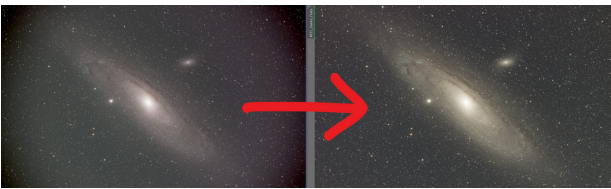


Figure 7. This image shows how the vignetting around the edges of the frame on the left are removed and the lighting is more uniformly distributed throughout the frame once the flat frame calibration is complete.

650 Arc frames, or arcs are used to convert the image pixels to  
651 wavelengths; they specify where the wavelength  
652 lines lie in the CCD. For this purpose, GMOS uses a  
653 Cu-Ar lamp, as multiple known emission lines across  
654 the range of the detector can be used to calculate the  
655 transformation between wavelength and pixel. Figure 8  
656 shows shows one of the arcs used for calibration in the  
657 DRAKE pipeline.

658 The last step is the flux calibration with the standard  
659 from the SSS. The SSS imaged for the standard is a  
660 nearby star with the same airmass as the target object.  
661 Reference SSS images, taken from across the nighttime  
662 sky, are stored for use when a new object in a particu-

<sup>15</sup> <https://astrojourneyuk.com/lights-darks-bias-and-flats-what-are-they-how-do-you-take-them-and-what-do-you-do-with-them>

663 lar area is found. The standard extracts the flux as a  
664 function of wavelength, as shown in Figure 9.

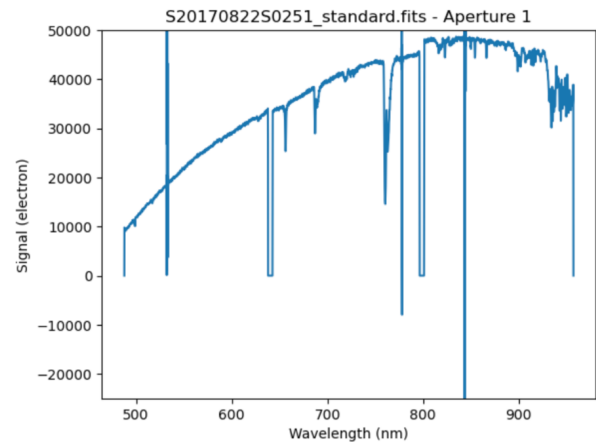


Figure 9. Standard Frame

665 In the DRAKE pipeline, lists of the biases, flats, arcs,  
666 and standards were created, separately. These biases,  
667 flats, arcs, and standards were later stacked together in  
668 their corresponding categories to form one master frame  
669 for each. A master bias, master flat, processed arc, and  
670 processed standard were created by stacking and averaging  
671 the respective frames, thus producing one image for  
672 each of the four calibrations. The Python `Reduce` class  
673 defined in DRAGONS handles the reduction of these  
674 frames.

#### 675 4.4. Spectrophotometric Star and Science Observation 676 Frames

677 The SSS is a reference star, imaged previously, to help  
678 calibrate the new, unstudied object. SSSs are imaged  
679 across the nighttime sky, and are stored for use when  
680 a new object in a particular area is found. Usually, the

681 SSS closest to the new object will be used for calibration  
 682 purposes. For DRAGONS pipelines such as this one, the  
 683 SSSs used by Gemini, are found in a “lookup table.”<sup>16</sup>  
 684 The SSS will be recognized by the Astrodata package as  
 685 a “standard”. The SOs are the images of the actual ob-  
 686 ject being analyzed, usually labeled as “object” or with  
 687 its object name (e.g. “NGC4993OT”). These files are  
 688 compiled in a new list of the SOs. The next step in the  
 689 pipeline was to download the BPMs and their associated  
 690 calibrations to the local calibration manager database<sup>16</sup>.  
 691 BPMs are handled like the calibrations previously dis-  
 692 cussed.

## 5. RESULTS

### 5.1. *J2145+0031 Results from the DRAGONS pipeline*

695 A 2D spectral image and a 1D calibrated flux spec-  
 696 trum were produced from Example One. Figure 10  
 697 shows the 2D image of the white dwarf candidate ob-  
 698 ject, J2145+0031, produced from the pipeline. This im-  
 699 age was displayed using DS9 astronomical imaging and  
 700 data visualization software. Ultimately, the pipeline in  
 701 Example one used biases, flats, and arcs to reduce the  
 702 2D image for a clearer and cleaner display of its asso-  
 703 ciated spectrum.

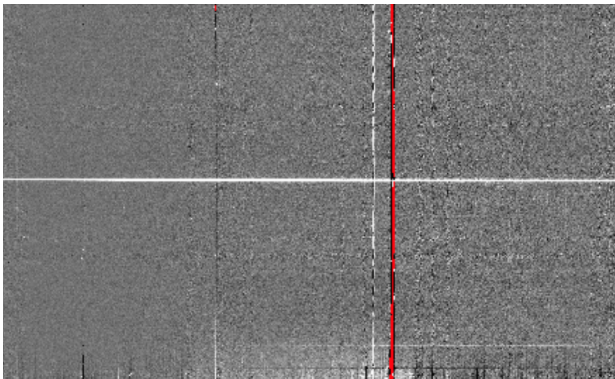


**Figure 10.** 2D image of the trace from white dwarf object J2145+0031.

704 After completing the pipeline from Example One, a  
 705 vertical slice of the 2D spectrum (Figure 10) was taken  
 706 using DS9, which is shown in Appendix 1. The peak  
 707 displayed in this plot represents the light coming from  
 708 the white dwarf candidate object: J2145+0031, gener-  
 709 ated as a result of the vertical slice. While a vertical  
 710 slice only shows the peak of where the spectrum is, a  
 711 horizontal slice will produce an entire spectrum with  
 712 absorption or emission lines corresponding to the object

<sup>16</sup> [https://dragons.readthedocs.io/projects/gmosls-drtutorial/en/v3.1.0/ex1\\_gmosls\\_dithered\\_api.html](https://dragons.readthedocs.io/projects/gmosls-drtutorial/en/v3.1.0/ex1_gmosls_dithered_api.html)

713 imaged. The plot in Appendix 1 is in counts average vs.  
 714 pixel.

715 The 1D spectrum data from Example One was opened  
 716 and displayed as a `numpy` array. The two columns of  
 717 data, wavelength and flux, were plotted. The flux data  
 718 needed to be fitted to a different scale in order to see  
 719 the spectrum better. After the x-axis (wavelength) was  
 720 adjusted to center the spectrum, while the best values  
 721 for the y-axis (flux) were found by trying various pa-  
 722 rameters until a clean graph was produced, as shown in  
 723 Figure 11. Some features, like the one around 570 nm  
 724 are likely the result of a bad pixel in the CCD.

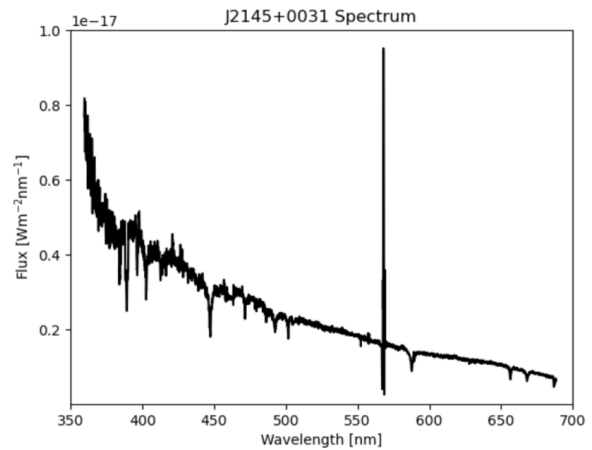


**Figure 11.** This image shows the flux of white dwarf object J2145+0031 as a function of wavelength.

725 After scaling this plot, the spectral line associated  
 726 with its absorption features were attained. Research was  
 727 done on spectral lines at the corresponding wavelengths  
 728 in Figure 12 and fitted to the spectrum. Many of the  
 729 lines were found using previous data recorded on Fritz.  
 730 Figure 12 shows the spectral lines and elements corre-  
 731 sponding to the spectrum for the white dwarf candidate  
 732 object: J2145+0031.

### 5.2. *GW170817 Results from the DRAKE pipeline*

734 The spectrum from GW170817 was reanalyzed using  
 735 the DRAKE pipeline previously discussed. The DRAKE  
 736 pipeline reduced and calibrated the GW170817 data,  
 737 performing bias subtraction, flat normalization, wave-  
 738 length calibration, and flux calibration, to create the  
 739 plot shown in Figure 13, which shows the raw spec-  
 740 trum for GW170817. In the raw spectrum, there still seemed  
 741 to be lingering contamination lines, represented with the  
 742 red arrows in Figure 13. Contamination lines were differ-  
 743 entiated from spectrum absorption features by searching  
 744 for spectral line broadening. With the target object’s

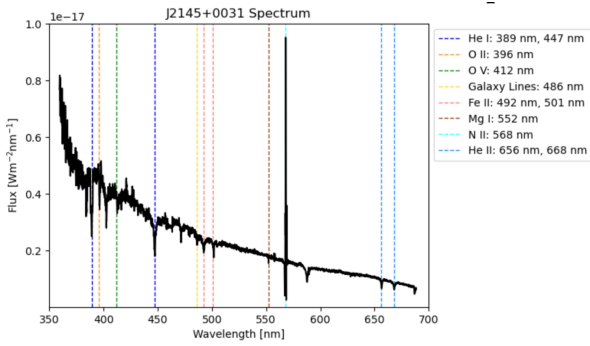


**Figure 12.** In this figure, spectral lines are overlaid on the plot corresponding to the white dwarf object J2145+0031 absorption spectrum.

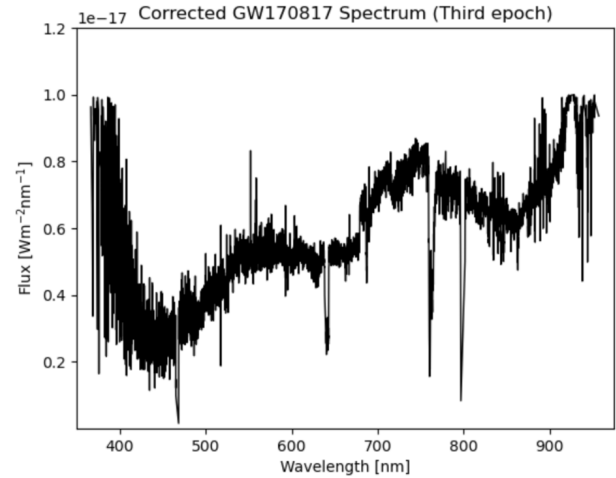


**Figure 14.** Corrected spectrum for GW170817

745 velocity, there will be spectral line broadening that cor-  
746 respond to the absorption lines on the spectrum.

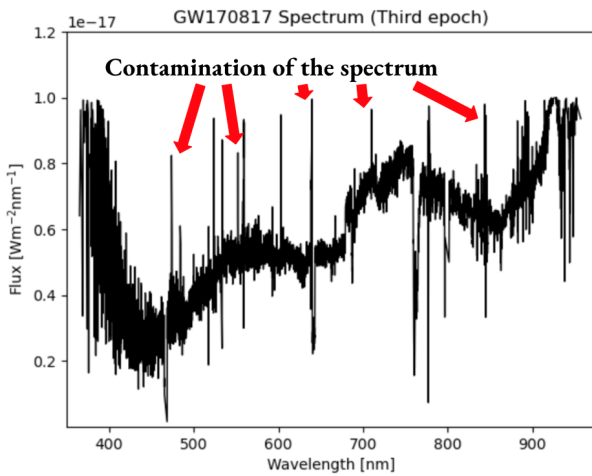


**Figure 13.** Raw spectrum for GW170817 with red arrows corresponding to the contamination of the plot.

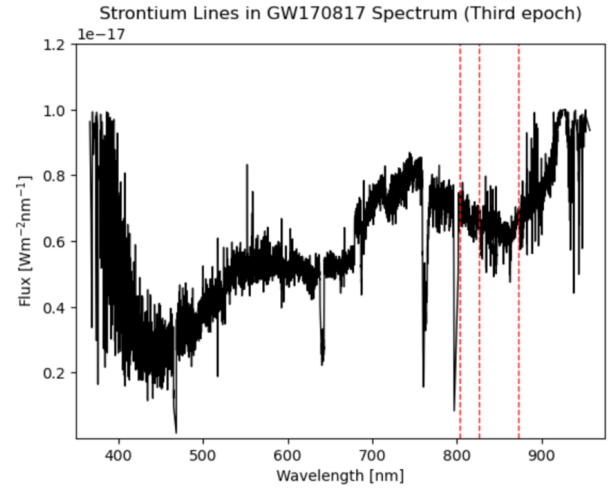


**Figure 15.** GW170817 spectrum with Strontium absorption features.

747 Figure 14 shows the GW170817 spectrum without the  
748 contamination, which was done by manually clipping  
749 each of the contamination lines.

750 The next task after recreating the GW170817 spec-  
751 trum was plotting specified absorption lines that could  
752 have occurred during the merger. In the Watson 2019  
753 paper, there is a large dip in the spectrum in both epoch  
754 2.5 and 3.5. Since the data used in this project was from  
755 the third epoch, this paper was a good reference to at-  
756 tempt to recreate these strontium absorption lines. The  
757 three strontium lines and the dip that was shown in the  
758 Watson 2019 paper were able to be reproduced in this  
759 project as shown in Figure 15.

760 Other spectral absorption lines mentioned in other  
761 published papers on GW170817 were also plotted on the  
762 spectrum produced in this project, as shown in Figure  
763 16. However, this is an ongoing process, and some tests

764 still need to be run before any more conclusions can be  
765 drawn about specifically what elements were produced  
766 in the GW170817 merger.

## 767 6. CONCLUSIONS AND FUTURE ENDEAVORS

768 The goals of this project were completed, including  
769 learning the DRAGONS pipeline, running the DRAG-  
770 ONS pipeline with sample data, adapting the DRAG-  
771 ONS pipeline to form the more generalized DRAKE  
772 pipeline, and reproducing the GW170817 spectrum and  
773 overlaying spectral lines. Future endeavors as related  
774 to this project could be to provide faster spectroscopic  
775 line identification for candidate vetting, to produce more  
776 consistent blackbody temperature estimation, to add  
777 current SN classification algorithms to the DRAKE  
778 pipeline, to provide a more in depth study of heavy ele-  
779 ment emission, and to classify more KN candidates.

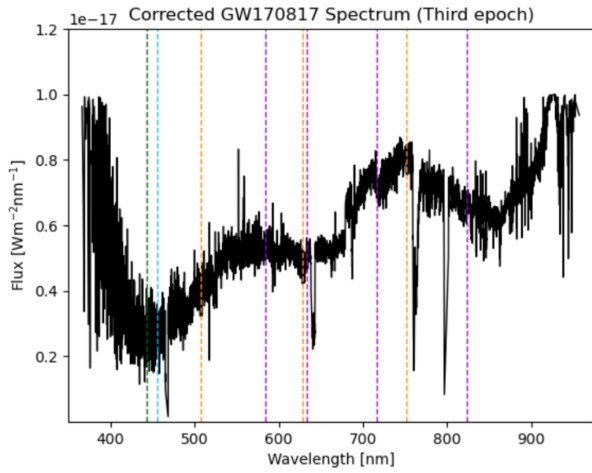


**Figure 16.** Platinum: purple, Selenium: blue, Tungsten: green, Gold: orange

## 7. ACKNOWLEDGMENTS

I would like to thank my mentors Tomas and Shreya, and supervisors Alan Weinstein and Mansi Kasliwal. We would like to thank the LIGO Laboratory and Caltech Student Faculty Programs office for the opportunity to participate in this SURF program and for their support throughout the summer. We thank the NSF REU program for their support.

## REFERENCES

- 780 Abbott, B. P., Abbott, R., Abbott, T. D., et al. 2017,  
781 PhRvL, 119, 161101
- 782 Ahumada, T., Anand, S., Coughlin, M. W., et al. 2022a,  
783 ApJ, 932, 40
- 784 —. 2022b, ApJ, 932, 40
- 785 Goldstein, A., Veres, P., Burns, E., et al. 2017, ApJL, 848,  
786 L14
- 787 Isoyama, S., Sturani, R., & Nakano, H. 2021, in Handbook  
788 of Gravitational Wave Astronomy, 31
- 789 Kasliwal, M. M., Anand, S., Ahumada, T., et al. 2020, ApJ,  
790 905, 145
- 791 Metzger, B. D. 2019, Living Reviews in Relativity, 23, 1
- 792 Perego, A., Thielemann, F. K., & Cescutti, G. 2021, in  
793 Handbook of Gravitational Wave Astronomy, 13
- 794 The LIGO Scientific Collaboration, the Virgo  
795 Collaboration, the KAGRA Collaboration, et al. 2021,  
796 arXiv e-prints, arXiv:2111.03606
- 797 Valeev, A. F., Castro-Tirado, A. J., Hu, Y. D., et al. 2021,  
798 in Revista Mexicana de Astronomia y Astrofisica  
799 Conference Series, Vol. 53, Revista Mexicana de  
800 Astronomia y Astrofisica Conference Series, 83–90
- 801 Watson, D., Hansen, C. J., Selsing, J., et al. 2019, Nature,  
802 574, 497

## 7. APPENDIX 1

803

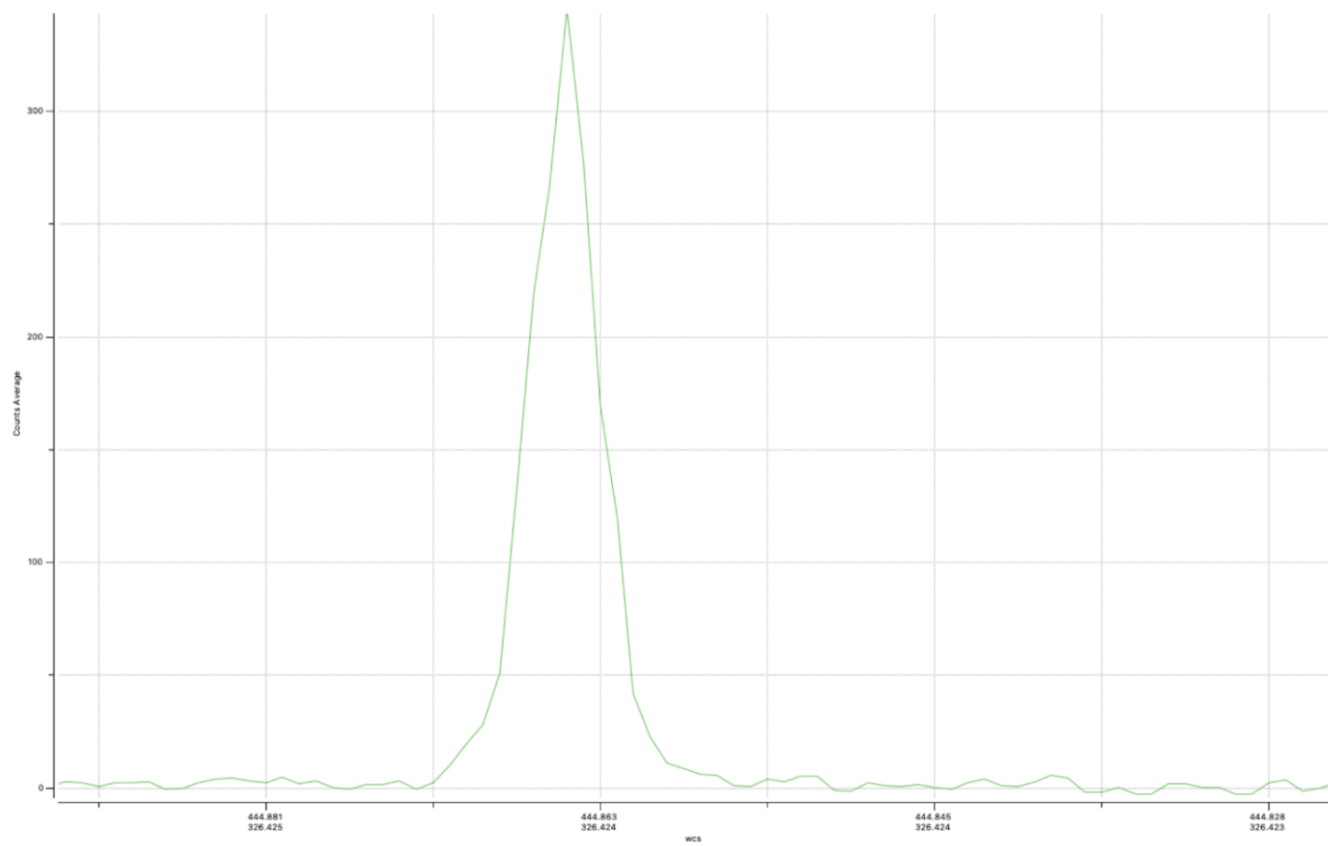


**Figure 17.** Slice of the spectrum from the white dwarf candidate object: J2145+0031.